substantially resembled those observed on the polycrystal. Fig. 144 shows the effect of previous compression on the limits of plasticity determined in the tensile test. The reduction of these limits well below their initial values by increasing compression appears very clearly.

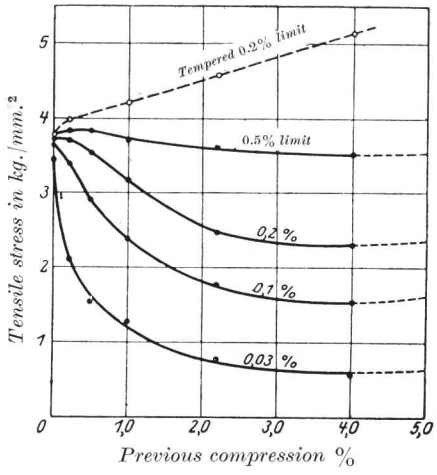

FIG. 144.—Effect of Previous Compression on the Limits of Plasticity of an α-Brass Crystal Subjected to Tensile Testing (290).

The importance of increasing the available experimental data on this subject must again be emphasized. It is particularly important for our conception of the fundamental processes involved to decide whether the freedom from after-effect and the occurrence of hysteresis in one and the same crystal material are really compatible with each other. An interpretation of the data presented here will be attempted in Section 76, while a discussion of these properties in relation to the technical polycrystal will be found in Section 82.

56. *Crystallographic Deformation and Cleavage Processes under Cyclic Stressing*

Experiments with cyclic stressing have been carried out on a large number of metal crystals. Usually the experiments have consisted of alternating-*torsion* tests on cylindrical specimens in which either the torque amplitude or the angle of torsion was maintained constant. Aluminium crystals were examined under tension–compression stress also. In the extensive series of tests by Gough the crystals were stressed in technical fatigue-testing machines. The specimens were here of the standard shape (cylindrical bar approx. 8 mm. in diameter, with thickened ends for clamping). The fatigue testing of thin crystal wires was carried out in suitably simplified machines, the angle of torsion being kept constant during the test. The number of stress reversals per minute in the various series of tests was 400–2300.

It should again be stated that an important result of these tests

was the establishment of the fact that the same glide and twinning elements operate under alternating as under static stress. *Aluminium* clearly shows glide bands which, in full agreement with the effects observed in tensile and compression tests, correspond to glide in the octahedral glide system as determined by the locally prevailing maximum shear stress [(292), (291)]. Therefore in alternating torsion the same glide system does not operate at all points on the circumference of the crystal. The transitions of the operative systems are often very clearly marked (see Fig. 145), and their positions always confirm the theoretical expectation.[1] The crystals fracture by forming cracks which in the main run along the operative glide planes (see Fig. 146). This is shown clearly by an alternating-torsion test carried out under tap water. The areas of maximum deformation are indicated by the greatly increased corrosion (cf. Fig. 147). In this test the effects of deformation and corrosion reinforce one another, and the fracture, which, in this case, occurs much earlier, is found to have occurred almost exclusively along the operative glide planes. This observation is important, because it shows that, contrary to the usual opinion, the cause of reduction of the fatigue strength under corrosive attack is not to be sought in the presence of stress concentrations at notches and holes (at any rate in so far as single crystals are concerned), but in the attendant crystallographic processes.

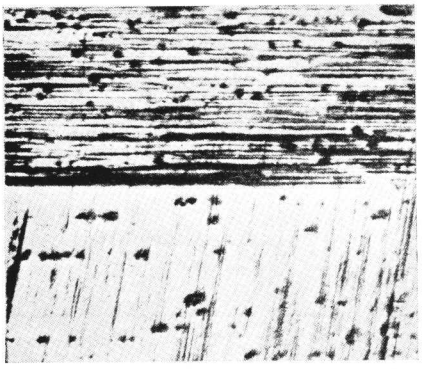

FIG. 145.—Transition of the Operative Glide Systems: Al Crystal Subjected to Alternating Torsion (292).

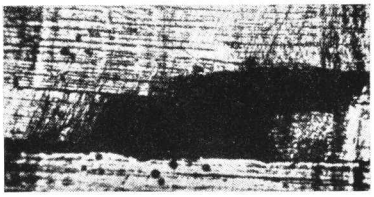

FIG. 146.—Fracture in an Al Crystal Subjected to Alternating Stress (291).

With a *silver* crystal, as in the case of aluminium, octahedral glide was observed after it had been subjected to torsional cycles. In this

[1] See Section 41 for a calculation of the shear stresses in the individual glide system.

case also the choice of the glide elements operative at various parts of the exterior of the crystal is determined by the condition of maximum shear stress; the resultant fracture again follows partially the operative glide planes. As with aluminium, mechanical twinning was not observed (295).

Magnesium crystals which had been subjected to alternating torsion exhibited both basal glide and the formation of deformation twins. The fractures are usually jagged and composed of several planes. Basal plane, prismatic plane $(10\bar{1}0)$, pyramidal planes $(10\bar{1}1)$ and $(10\bar{1}2)$, etc., have been observed as cleavage planes (296).

With *zinc* crystals, too, the same mechanisms of deformation

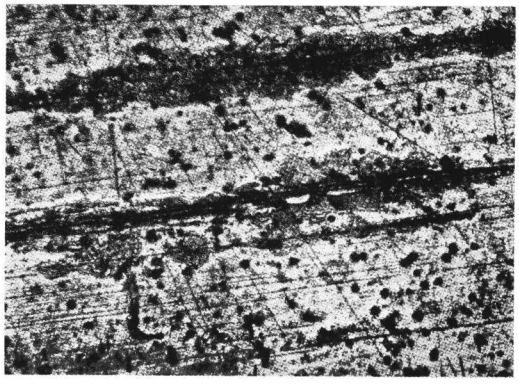

FIG. 147.—Fracture Produced in an Al Crystal by Corrosion Fatigue (294).

usually appear in alternating torsion as in the static tensile test, namely, glide in the basal plane and mechanical twinning with $K_1 = (10\bar{1}2)$. Dependent on the crystal orientation, several types of cracks accompany the traces of these crystallographic deformations. They result from cleavage along the basal plane, the secondary basal plane in twin lamellæ and also along the twin plane. Part of such a crack, composed of consecutive primary and secondary basal planes, is illustrated in Fig. 148. With this are associated cracks which follow the prism planes. These, however, are not so much fissures as flat troughs enclosed within swellings, although it is true that, after appreciable deformation, cracking makes its appearance at the bottom of the troughs (see Fig. 149). The crystals then fracture either by smooth cleavage along a primary or secondary

basal plane, or stepped fractures occur, in which, however, the basal plane is always involved [(298), (297), (299)]. Both the striations

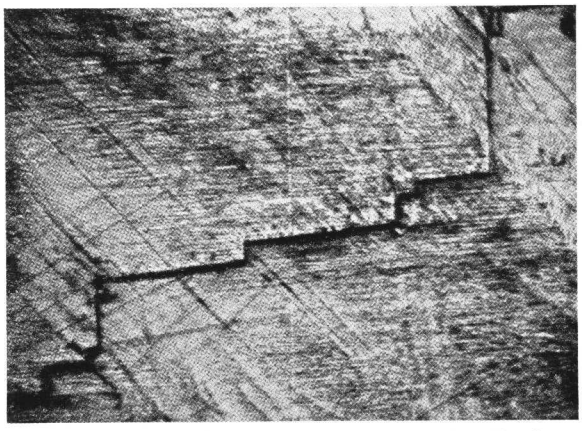

FIG. 148.—Zn Crystal Subjected to Alternating Torsion : Fracture along the Primary Basal Plane, and along a Secondary Basal Plane in Twin Lamellæ (298).

observed on the surface of *cadmium* crystals subjected to alternating torsion, and the change of the shape of the sections of these crystals

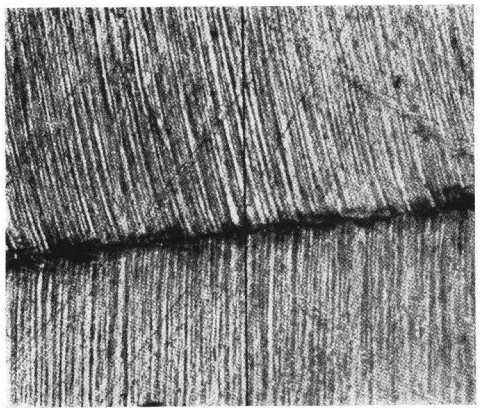

FIG. 149.—Fracture along Prism-plane Type II in a Zinc Crystal Subjected to Alternating Torsion (298).

(rib formation), were found by analysing the state of stress to be basal glide (300).

An *antimony* crystal exhibited no glide bands in alternating torsion, but deformation twins appeared on all three (011) planes. Secondary twinning was observed within the twin lamellæ. Crack formation and fracture followed definite crystal planes, as was indeed to be expected with a crystal having such good cleavage as antimony. The first cracks ran parallel to the (111) plane in its original or twinned position. Fracture occurred finally by cleavage about a twin plane (301).

Glide could no more be detected in *bismuth* crystals subjected to alternating torsion than in antimony. Numerous deformation twins on the (011) planes made their appearance in the first stages of the test. The cracks were oriented mainly parallel to the twinned (111) plane. Fracture occurred by cleavage along the basal plane (111) or along a plane which cannot be expressed by simple indices (302).

In conclusion, attention must also be drawn to the important fact that cracking under cyclic stressing is not confined to the crystallographic cleavage planes, but can also occur on a large scale along operative glide planes. This phenomenon points clearly to a close connection between the fatigue fracture of the single crystals and the deformation by which it was preceded.

57. *Phenomena of Hardening under Cyclic Stressing*

The crystallographic processes which attend the cyclic stressing of metal crystals were described in the previous section. Attention has already been drawn to the dynamics of these tests when discussing the initial conditions of twinning (Section 51). The present section will deal with the changes in the mechanical properties of crystals brought about by cyclic stressing. It will be seen that these changes are of a very marked and special nature, and they reveal the profound influence exerted by this type of stressing.

It can already be concluded from the development in time of glide bands in *aluminium* crystals under alternating stress that a substantial *shear hardening* must take place (291). This hardening seems to be less pronounced in the principally affected octahedral systems, which are characterized by maximum shear stress, than in the others, since the glide which takes place initially on several systems is soon restricted to the one which is most favourably placed. The non-equality of hardening, therefore, is of the same kind as in static tensile tests (Section 43).

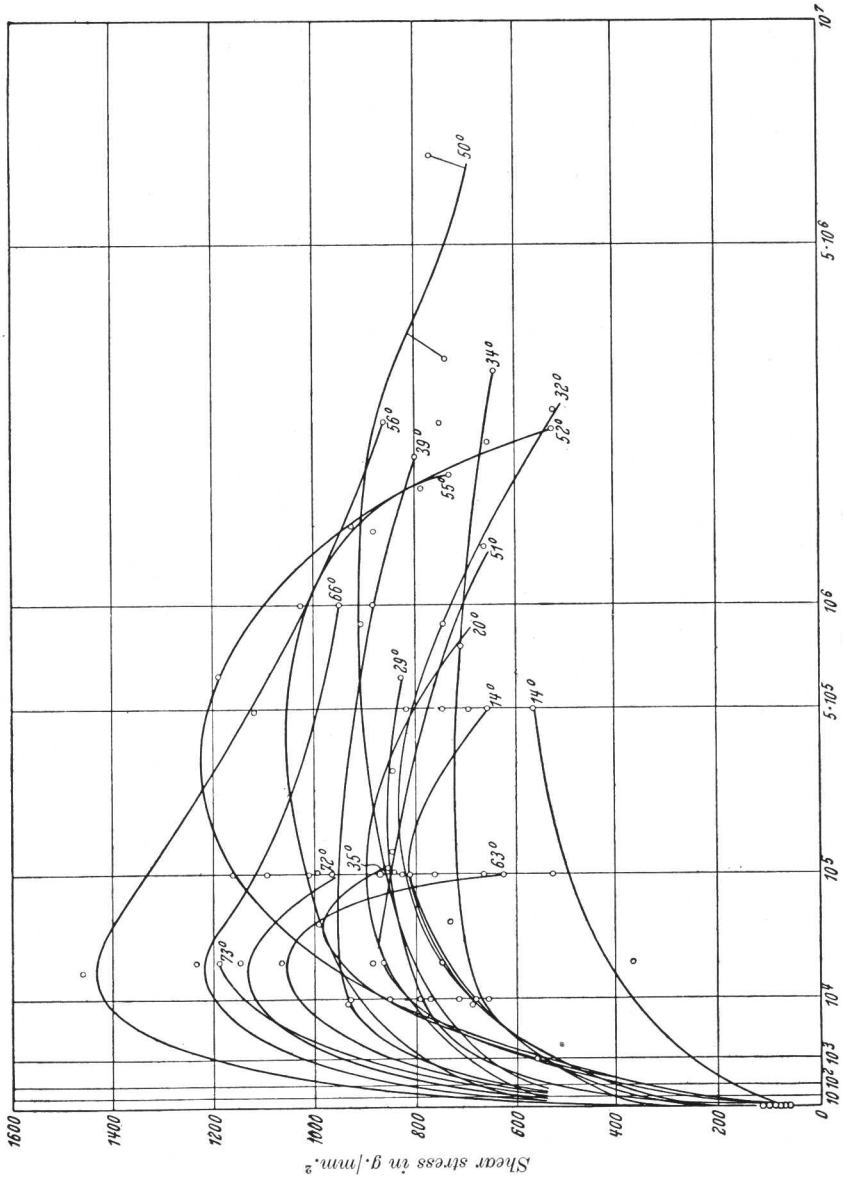

FIG. 150.—Shear Stress on the Basal Plane of Zn Crystals Subjected to Alternating Torsion (299). Angle of the Basal Plane Indicated in Each Case.

Hardness measurements at various points on the cross-section of an *aluminium* crystal, which had been subjected to alternating torsion to the point of fracture, reveal clearly a hardening in those areas which had experienced strong deformation. The hardness values obtained by ball impressions exceeded by 30–40 per cent. those obtained in the central undeformed zone (292).

The changes in the mechanical properties of *zinc* crystals were investigated directly [(297), (299)]. Thin crystal wires (approximately 1 mm. in diameter) were subjected to alternating torsion with a constant angular amplitude over varying numbers of stress reversals, followed by static tensile testing. Up to seven test specimens could be taken from one original crystal. Fig. 150 shows the shear stress of the basal glide system after alternating torsion by 4° in either direction (gauge length 40 mm.) as a function of the number of stress reversals. From this it will be seen that in every case the yield stress increases after a few stress reversals to many times its initial value (of approx. 90 g./mm.^{2}) and that it falls again *after reaching a maximum value*. Relatively to each other the curves scatter very considerably, but it will be noticed that those of the transversely oriented crystals are in the upper part of the scatter zone, while those of longitudinal orientations appear in the lower part. Similar results were obtained with magnesium crystals (296). Thus in contrast to the independence of the critical shear stress upon orientation in the undeformed state, after identical alternating stressing the shear stress seems to increase with increasing angle between the basal plane and wire axis.

The dependence of the critical normal stress of the basal cleavage plane upon the number of stress reversals was determined by fracturing the stressed crystal pieces at −185° C. in order to avoid the extensions which usually occur in tension at room temperature. The normal stress which is shown in Fig. 151 as a function of the number of reversals reveals, in general, a behaviour similar to that of the shear stress; it increases steeply to a maximum, but falls away again as the number of reversals increases. The dependence of the strain strengthening upon orientation also appears to resemble that of the shear hardening; as the angle of the basal plane increases so, too, does the maximum normal stress. At identical orientations the maximum values for shear and normal strength occur after the same number of reversals.

Whereas, therefore, cyclic stressing initially causes a substantial *hardening* and strengthening, in the further course of stressing a new phenomenon which leads to the *softening* and weakening of the

crystal becomes increasingly predominant. That the process which causes this weakening should be sought preferably in the lattice and not merely in the appearance of microscopic cracks, may be inferred from the circumstance that the maximum strength of the crystal is attained long before the appearance of visible cracks. Moreover, the fact mentioned above that other metals form cracks along

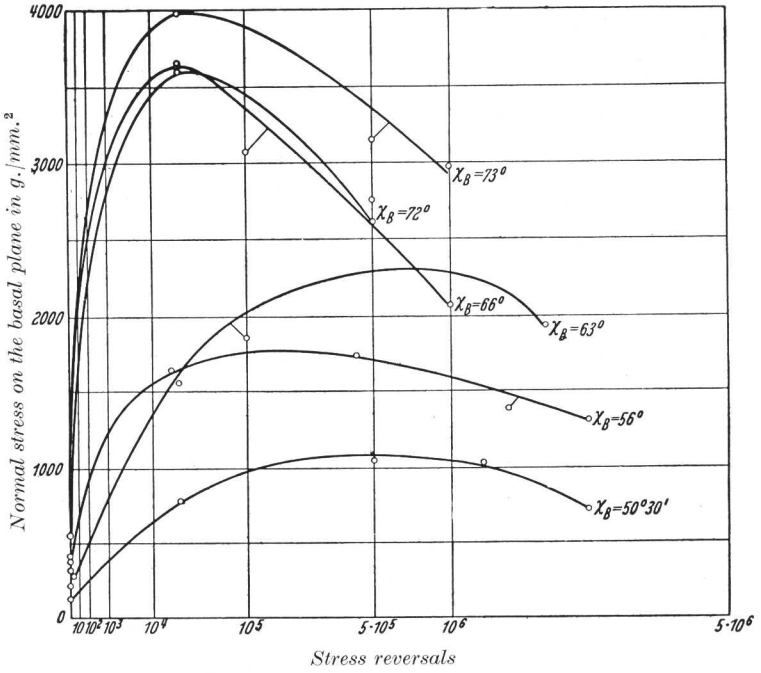

FIG. 151.—Normal Stress on the Basal Plane of Zn Crystals Subjected to Alternating Torsion (299).

operative glide planes which exhibit no cleavage in the undeformed crystal, points to a weakening of the glide planes (cf. also 293).

It follows from this that the fatigue strength of crystals may be defined physically as the stress at which, after an infinite number of reversals, the maximum of the mechanical properties is not exceeded. Statistical details of the fatigue strength of crystals are not yet available. In particular, the question of the relationship between orientation and fatigue strength is still open (cf. Section 82).

So far we have discussed the start of plastic extension and the

brittle fracture of cyclically stressed zinc crystals at low temperatures. Investigations of the *capacity for plastic deformation* at room temperature revealed a state of affairs which, in its essential characteristics, is illustrated in Fig. 152. First of all it will be noticed that with an angle of torsion approximately twice that adopted in the tests already described, the dependence of the yield stress on the number of stress reversals (to which reference has

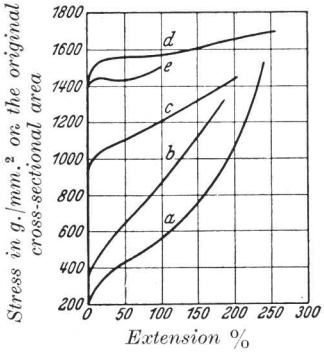

FIG. 152.—Stress–Strain Curve of a Zn Crystal after Varying Numbers of Stress Reversals (Torsion) (297). (*a*) After 0, (*b*) after 100, (*c*) after 1000, (*d*) after 10,000, and (*e*) after 50,000 twists (within an angle of 15°).

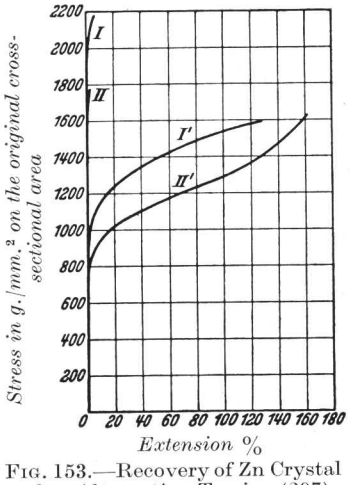

FIG. 153.—Recovery of Zn Crystal after Alternating Torsion (297).

I stress–strain curve after about 80,000 twists (within an angle of 20°); I′ after subsequent recovery over a period of 4 days (20° C.); II after about 140,000 twists; II′ after subsequent recovery over a period of 2 days (20° C.).

already been made) is again substantially the same. Up to 10,000 reversals, the capacity of the crystal for extension is by no means reduced; only after 50,000 twists does it fall to about one half. Where the angles of torsion are smaller, and the basal plane is not too oblique, no decrease in extension is observed even after many millions of reversals. At this number of reversals the shear-strength maximum has long since been exceeded. The further hardening by plastic extension, which is expressed in the inclination of the curves, diminishes noticeably as initial cyclic stressing increases. Here again we confront the fact, to which attention has been repeatedly drawn, that with increasing primary hardening

[formation of solid solution, appreciable shear hardening of an initially latent glide system (Section 46) mechanical twinning (Section 52)] further capacity for hardening by deformation is progressively reduced.

If the cyclic stressing of the crystals is carried very far, circumstances may arise in which brittleness will occur in the tensile test even at room temperature, depending on the orientation of the crystal. Crystal recovery causes this brittleness to disappear and a crystal subjected to alternating torsion attains very nearly its original plasticity. Fig. 153 illustrates this by two examples. The capacity for recovery, together with the already mentioned retention of ductility in certain cases, conflicts with the view that the formation of cracks is entirely responsible for the observed weakening in the later stages of the fatigue test.

Two remarks remain to be made. First, in the alternating-torsion test it is not the whole section of the crystal which is deformed but only a relatively thin surface layer. Therefore, since tubular test specimens were not employed, the shear and tensile stresses obtained in the static tensile test with cyclically stressed crystals represent only the average values for the more or less deformed portions of the crystals. Consequently the changes in the mechanical properties which actually occur in the deformed zone are greater than those shown here. Secondly, when the same zinc crystal is subjected to torsion and subsequent extension it is not usually the same digonal-axis type I which becomes effective as a glide direction. Owing to cyclic deformation, glide on the basal plane, which is always the operative glide plane, is also greatly hampered in initially latent directions.

F. CHANGE IN PHYSICAL AND CHEMICAL PROPERTIES BY COLD WORKING

In the preceding sections we dealt with the crystallographic laws governing the plastic deformation of crystals, and the dynamics of the processes themselves. The appreciable changes produced in the mechanical properties by plastic deformation (hardening) have already been discussed. But deformation also modifies to a greater or lesser extent most of the other physical and chemical properties of the crystals.

In regard to the directional properties, an important distinction must here be made between the changes resulting from cold working as such, and those due to the re-orientation of the crystal in the course of deformation. If it is desired to ascertain solely the effect

of cold working, allowance must always be made for the changes resulting from lattice rotation in interpreting the observed effects.

TABLE XVIII

Elastic Coefficients of Metal Crystals (10^{-13} *cm.²/Dyn.*)

Metal.	s_{11}.	s_{12}.	s_{44}.	s_{13}.	s_{33}.		Literature.
Aluminium	15·9	− 5·80	$35{\cdot}1_6$	—	—	—	(6)
Al + 5% Cu	15	− 6·9	37	—	—	—	(303)
Copper	15·0	− 6·3	13·3	—	—	—	(7)
Silver	23·2	− 9·93	22·9	—	—	—	(8)
Gold	24·5	− 11·3	25	—	—	—	(6)
	22·7	− 10·35	22·9	—	—	—	(8)
Ag + 25 At.-% Au	20·7	− 8·91	20·52	—	—	—	(8)
Ag + 50 At.-% Au	19·7	− 8·52	19·66	—	—	—	
Ag + 75 At.-% Au	20·5	− 9·09	20·63	—	—	—	
α-Brass (72% Cu)	19·4	− 8·35	13·9	—	—	—	(9)
α-Iron	7·57	− 2·82	8·62	—	—	—	(10)
Tungsten	2·534	− 0·726	6·55	—	—	—	(11)
	2·573	− 0·729	6·604	—	—	—	(12)
Magnesium	22·3	− 7·7	59·5	− 4·5	19·8	—	(13)
	20·4	− 5·2	87·8	− 5·2	20·4	—	(14)
Zinc	8·4	1·1	26·4	− 7·75	28·7	—	(15)
	8·23	0·34	25·0	− 6·64	26·38	—	(11)
Cadmium	12·3	− 1·5	54·0	− 9·3	35·5	—	(15)
	12·9	− 1·5	64·0	− 9·3	36·9	—	(11)
Bismuth	26·9	− 14·0	104·8	− 6·2	28·7	s_{14} = 16·0	(11)
Antimony	17·7	− 3·8	41·0	− 8·5	33·8	s_{14} = − 8·0	
Mercury *	154	−119	151	−21	45	s_{14} = − 100	(304)
Tellurium	48·7	− 6·9	58·1	−13·8	23·4	s_{14} = ?	(11)
β-Tin	18·5	− 9·9	57·0	− 2·5	11·8	s_{66} = 135	

* At −190° C.

TABLE XIX

Maximum and Minimum Values for Young's Modulus and the Shear Modulus of Metal Crystals

Metal.	$E_{max.}$		$E_{min.}$		$G_{max.}$		$G_{min.}$	
	kg./mm.².	Direction.	kg./mm.².	Direction.	kg./mm.².	Direction.	kg./mm.².	Direction.
Aluminium	7,700	[111]	6,400	[100]	2,900	[100]	2,500	[111]
Copper	19,400		6,800		7,700		3,100	
Silver	11,700		4,400		4,450		1,970	
Gold	11,400		4,200		4,100		1,800	
α-Iron	29,000		13,500		11,800		6,100	
Tungsten	40,000		40,000		15,500		15,500	
Magnesium	5,140	0° *	4,370	53·3°	1,840	44·5°	1,710	90°
Zinc	12,630	70·2°	3,560	0°	4,970	90°	2,780	41·8°
Cadmium	8,300	90°	2,880	0°	2,510	90°	1,840	30°
β-Tin	8,640	[001]	2,680	[110]	1,820	45·7° †	1,060	[100]

* Angle with the hexagonal axis.
† Angle with the tetragonal axis in prism plane type II.

In the first place, therefore, we will consider the possible extent of the effects of orientation.

58. *Anisotropy of the Physical Properties of Metal Crystals*

The dependence upon orientation of Young's modulus and of the shear modulus has already been expressed, in Section 10, by the equations (10/1, 2) and (10/4, 5) for the case of cubic and hexagonal crystals. With regard to the specific electrical resistance, the cubic crystals are isotropic. Hexagonal, trigonal and tetragonal crystals exhibit axially symmetrical behaviour with respect to the principal axis. If ϕ is the angle formed by the investigated direction with the c axis, then the specific resistance ρ is expressed by—

$$\rho = \rho_{\perp} = (\rho_{\parallel} - \rho_{\perp}) \cdot \cos^2 \phi \quad . \quad . \quad . \quad (58/1)$$

$\rho_{\perp}$ and $\rho_{\parallel}$ signify the specific resistance perpendicular and parallel to the principal axis. The same dependence upon orientation applies to the specific resistance ω for the thermal conduction,[1] to the coefficient of thermal expansion α, to the thermoelectric power e,[2] to the constant σ of the Thomson-effect,[3] and to the magnetic susceptibility κ.[4] In respect of all these properties cubic crystals are isotropic; in crystals with a principal axis (hexagonal, trigonal, tetragonal) the value of the property in question, in any direction whatsoever, is represented by two constants (the values parallel and perpendicular to the principal axis) and by the angle formed by the direction investigated with the c-axis, in accordance with the above formula.

Tables XVIII–XX contain a summary of the values so far obtained for metal crystals. A graphical representation of the anisotropy of Young's modulus and the shear modulus is found in Fig. 154, *b* and *c*.

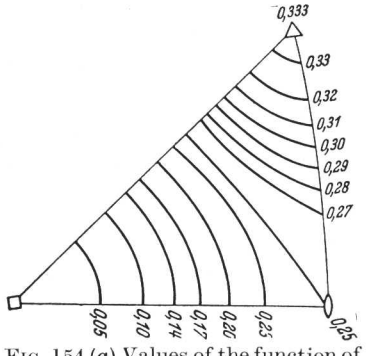

FIG. 154 (*a*) Values of the function of orientation $(\gamma_1^2\gamma_2^2 + \gamma_2^2\gamma_3^2 + \gamma_3^2\gamma_1^2)$ in the equations (10/1, 2) for cubic crystals.

---

[1] $\omega = \frac{1}{\lambda}$; λ = thermal conductivity, *i.e.*, the quantity of heat which flows per second through a unit section of the conductor with a temperature gradient of 1° C. per cm.

[2] Thermoelectric power against a standard metal (*e.g.*, copper) when the difference in temperature at the two junctions is 1°.

[3] σ is the heat developed in 1 cm. of conductor by the passage of 1 unit of electricity at a temperature gradient of 1° per cm.

[4] $\kappa = \frac{M}{H}$, when M represents the magnetic moment produced in the unit volume through a magnetic field of intensity H.

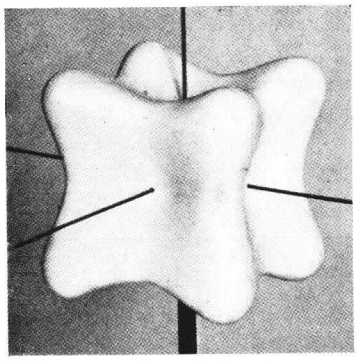

Young's modulus, Au

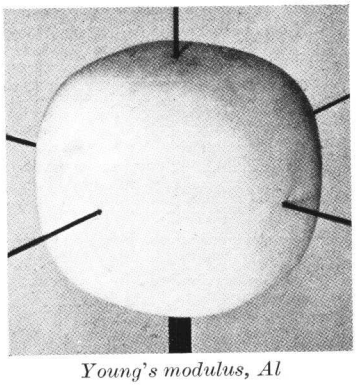

Young's modulus, Al

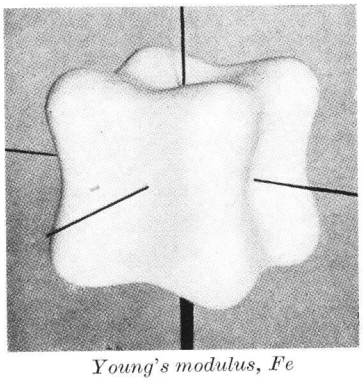

Young's modulus, Fe

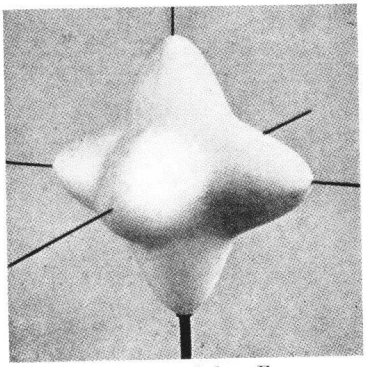

Shear modulus, Fe

(*b*) Young's modulus and shear modulus surfaces of cubic crystals (10).

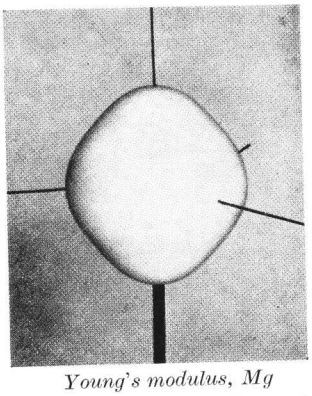

Young's modulus, Mg

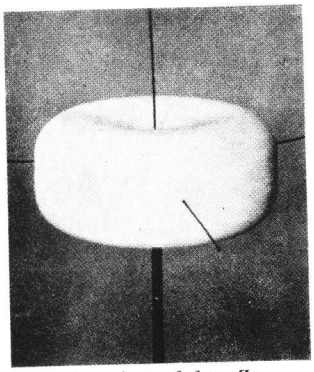

Young's modulus, Zn

(*c*) Young's modulus surfaces of hexagonal crystals (305).

FIG. 154 (*a*)–(*c*).—Elastic Anisotropy of Metal Crystals.

o

TABLE

Anisotropy of the Physical Pro

Metal.	Specific electrical resistance, 10^{-6} Ω/cm.			Specific thermal conductivity, watt/cm., ° C.		
	∥.	⊥.	Literature.	∥.	⊥.	Literature.
Magnesium	3·80	4·58	(306)	—	—	—
	3·85	4·55	(307)	—	—	—
Zinc	6·06	5·83	(309)	1·24	1·24 *	(309)
	6·13	5·91	(311)	—	—	—
Cadmium	8·36	6·87	(309)	0·83	1·04	(309)
	8·30	6·80	(311)	—	—	—
Mercury †	0·0557	0·0737	(315)	0·399	0·290	(316)
Bismuth	138	109	(304)			
Antimony	35·6	42·6	(311)	—	—	—
Tellurium	56,000	154,000				
β-Tin	14·3	9·9				

* At −252° C.; 7·09 or 5·65.
† All measurements at −188° C.

A further property, not referred to in the tables, is the rate of solution. This, too, depends substantially on the crystallographic

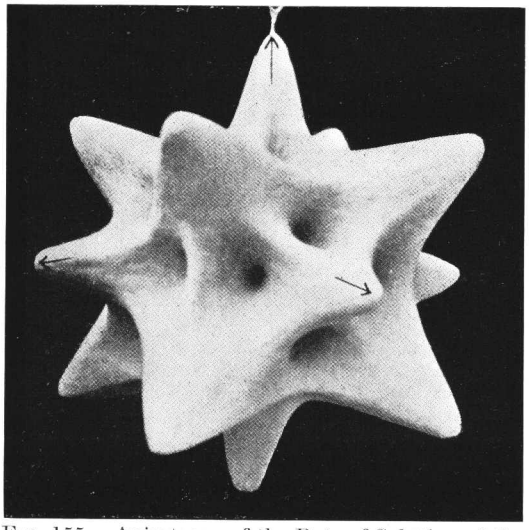

FIG. 155.—Anisotropy of the Rate of Solution of the Copper Crystal in Acetic Acid (317).

direction. With cubic metals it may vary very considerably, as is seen from Fig. 155. The directions of maximum rate of solution,

XX

perties of Metal Crystals (at 20° C.)

Thermal expansion, 10^{-6}.				Thermoelectric force compared with copper, 10^{-6} V/° C.			Thomson effect 10^{-6}, cal./coul. ° C.		
Temp. range, ° C.	∥.	⊥.	Literature.	∥.	⊥.	Literature.	∥.	⊥.	Literature.
20–100	26·4	25·6	(306)	1·87	1·66	(308)	—	—	—
about 20	27·1	24·3	(308)	—	—	—	—	—	—
20–100	63·9	14·1	(310)	1·32	− 0·50 ‡	(312)	0·34	0·86	(313)
about 20	57·4	12·6	(311)	—	—		—	—	—
20–100	52·6	21·4	(310)	1·60	− 1·74		1·64 §	1·96	(314)
−188 to −79	47·0	37·5	(304)	−17·9¶	−15·1	(316)	—	—	—
about 20	14·0	10·4	(311)	—	—	—	—	—	—
	15·6	8·0							
	−1·6	27·2							
	30·5	15·5							

‡ The minus sign shows that the current at the cold junction is flowing towards the copper.
§ Determined at 100° C.
¶ Measured against constants.

however, are by no means always the same; the nature of the solvent is of decisive importance [cf. (318), (319)]. Among hexagonal metals the anisotropy of the rate of solution has so far been investigated in the case of magnesium only (320).

If it is desired to examine the effect of cold work upon the physical properties of a polycrystalline material, then only non-directional properties should be measured directly. Otherwise attention must be paid to the development of deformation textures, that is, to the preferred orientations which result from deformation (see Section 78). This orientation effect is superimposed upon the actual change in the properties which has been produced by cold working. Several investigations into the effect of cold deformation on polycrystals have to-day lost much of their value through neglect of this fact, the significance of which has been recognized only in the past fifteen years.

59. *Cold Work and the Crystal Lattice*

The mere fact that, even after very appreciable distortion, the deformation of crystals is strictly determined by crystallographic factors, is a clear indication that the lattice structure is essentially retained during cold working. This has been proved quantitatively by measurements of the symmetry and parameters of the lattice. Fig. 156 shows by way of example Debye–Scherrer diagrams of

copper in the form of fine-grained casting, and of wire subjected to maximum cold working; in both cases the position of the lines is identical. Exact determinations of the lattice constants show that their value varies less than 1 part per thousand even after very substantial deformation (Al, Zn, Cu).

It is true that the diagrams of both single and polycrystals in the cold deformed state reveal changes which indicate that the lattice structure is to some extent influenced by deformation. In the diagrams obtained with monochromatic X-rays these differences

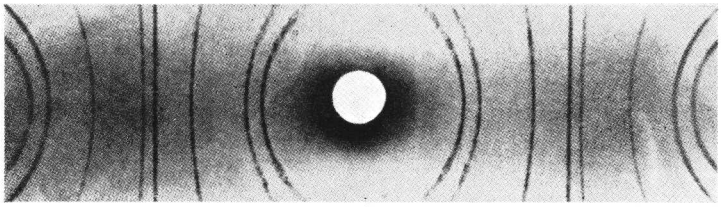

(*a*) Cast.

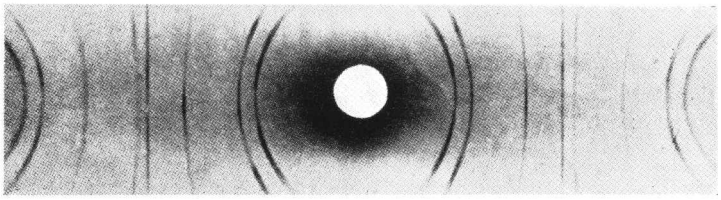

(*b*) Wire drawn cold to nearly 2000 times the original length.

FIG. 156 (*a*) and (*b*).—Retention of the Lattice Structure During Cold Working. Debye–Scherrer Patterns of Copper (see 321).

relate to both the length of the X-ray reflexions and to some extent to their width and intensity also. In the Laue diagrams of deformed crystals obtained with " white " X-rays, long distorted spots appear (asterism) (see Fig. 157).

The *lengthening* of the reflexions in the rotation photographs of deformed single crystals indicates the presence of positions which differ from the lattice positions as determined theoretically from the initial position and the degree of deformation. Investigations on aluminium crystals have shown that these deviations from the theoretical position are due to a rotation about an axis which lies in an operative glide plane perpendicular to the glide direction (323). This may be a consequence of a bending of the crystal or of a rotation of separate crystal fragments. In the Laue diagram a *streak-shaped*

distortion of the reflexions along curves of the fourth order is to be expected from a lattice curvature (Fig. 158); in fact, the observed asterism conforms entirely to this expectation [(324), (325)].[1] The

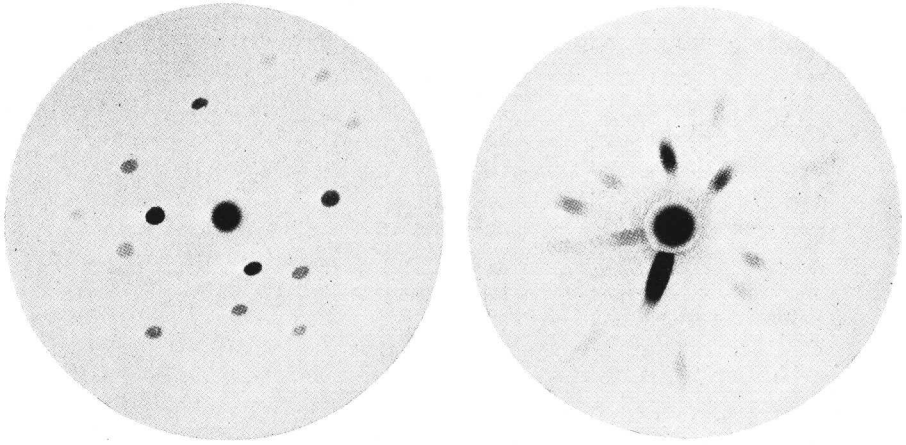

(*a*) Unstressed Al crystal. (*b*) The same crystal after extension (20%) and rolling down by about 30%.

FIG. 157 (*a*) and (*b*).—Asterism in a Laue Photograph of a Deformed Crystal (322).

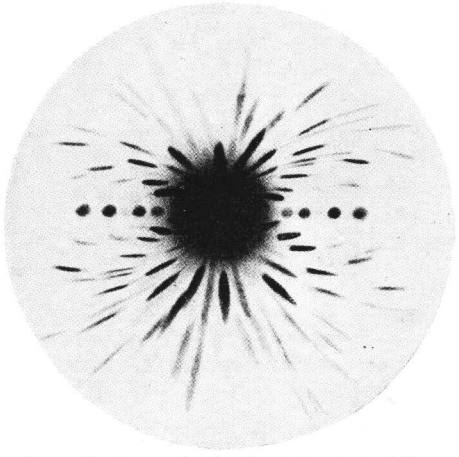

FIG. 158.—Laue Photograph of a Bent Crystal of Gypsum (326).

frequency of the positions diminishes rapidly as the distance from the theoretical orientation increases; the maximum of the deviation

[1] For special positions of the axis of bending in relation to the incident ray, cf. (327) and (328).

increases with the extent of the glide. The curvature does not greatly exceed 20°. If multiple glide occurs in the further course of the deformation, several axes of rotation become available for the displacement of the lattice components (329). If deformation is

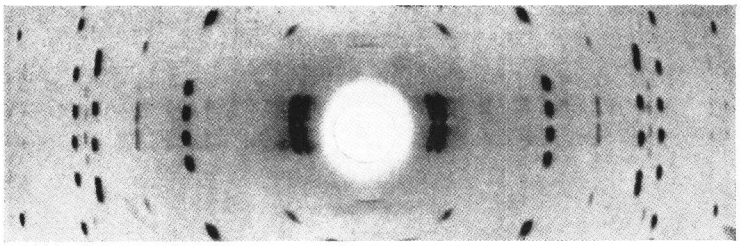

(*a*) Initial state, high angle lines θ.

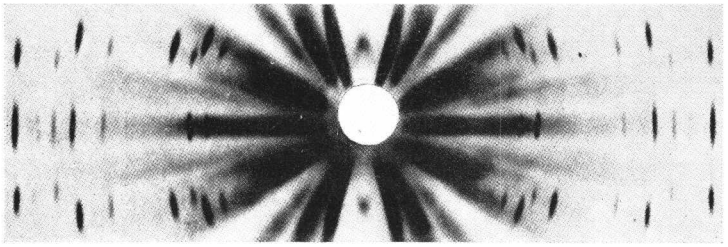

(*b*) Fractured specimen, low angle lines θ.

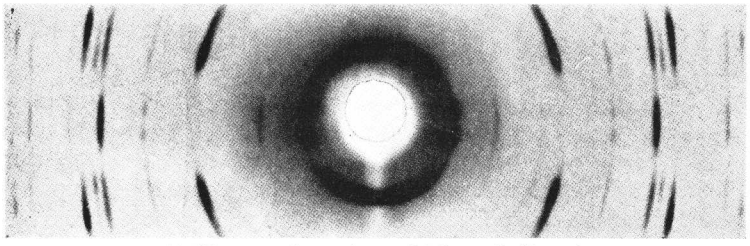

(*c*) Fractured specimen, high angle lines θ.

FIG. 159 (*a*)–(*c*).—Divergences from the Theoretical Position of the Lattice in an Extended Al Crystal. Rotation photographs, Cu-radiation.

followed by reverse deformation the asterism is again reduced in spite of increased hardening (330). The divergencies from the theoretical position of the lattices are particularly noticeable for reflexions with large angles of deviation.[1] This is illustrated in

[1] It follows from the differentiation of formula (19/1) that for a given angular range of the normal of the reflecting plane, the length of the reflected spot increases with the angle of reflexion.

Fig. 159 by rotation photographs of an extended aluminium crystal, and in Fig. 160 by Laue photographs of the same crystal; in the back-reflexion photographs the effect of the curvature is stronger.

The *broadening* of X-ray diffractions has been studied mainly with polycrystalline material [(331), (332), (333)], but this effect makes its appearance also in single crystals. It is found only in high angle lines where it is observed as a diffusion of the K_α doublet (see Fig. 161). This broadening of the lines increases mainly at the start of deformation with increasing degree of working [(334), (335)]; however, it by no means attains the same magnitude with

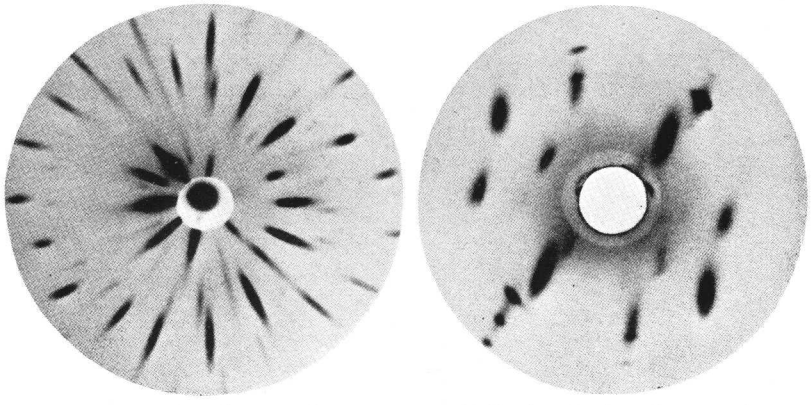

(*a*) Transmission photograph. (*b*) Back-reflexion photograph.

FIG. 160 (*a*) and (*b*).—Laue Photographs of an Extended Al Crystal.

all metals. Whereas with iron, copper, silver, tungsten and platinum, considerable diffusion is observed, with aluminium and zinc the doublet lines remain clearly separated even after strong deformation. Reduction of the temperature of deformation, however, results in distinct broadening of the lines in the case of aluminium (336). Alloys of aluminium in the quenched and heat-treated state exhibit very substantial broadening of the lines and reduction of their intensity even after small deformations (337). Just as the orientation of the grains differs in the different layers of cold-worked components (cf. Section 78) so too does the broadening of the X-ray-diffraction lines (338).

There are three possible explanations of the broadening of the lines as a result of cold working.

1. *Elastic distortion* caused by internal stresses (Heyn's residual stresses) which, *over sufficiently large volumes*, produce approximately

constant lattice spacings, although of slightly different value from the original. These divergencies occur in both directions; the volumes within which the stress is approximately constant must be sufficiently large to produce visible interferences (approx. 0·5 μ) (cf. also Section 82).

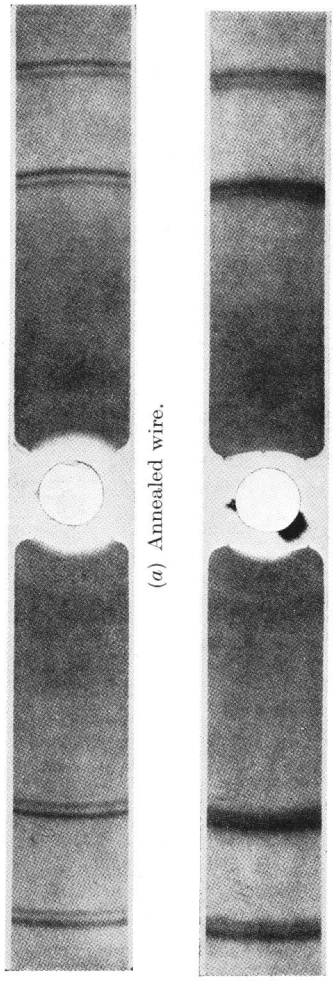

(*a*) Annealed wire. (*b*) Cold-drawn wire.

Fig. 161 (*a*) and (*b*).—Broadening of the X-ray Diffraction Rings by Cold Working. Exemplified by Copper (see 321).

2. *Fragmentation.* A broadening of the lines becomes perceptible at grain sizes below approximately 10^{-5} cm.

3. *Inhomogeneous distortions of the lattice* (warpings, strong distortions within the intact lattice). The calculation of models representing this type of lattice disturbances revealed that their effect on the width of the line depends largely on the type of disturbance assumed; lattice bending leads to a broadening; if, on the other hand, the distortions are partial and periodic, so that less than half of the lattice points are shifted from their normal position, then as a rule there will be no change in the definition of the lines. Broadening on this assumption differs fundamentally from that arising out of assumption 1. Whereas in that case broadening is due to normal diffraction in large volumes, with which only a slightly changed lattice constant is associated, in the present case it is explained by the super-imposing of "ghosts" upon the normal diagram. The intensity of these new lines, caused by the periodicity of the disturbances, is particularly great in the neighbourhood of the original Debye–Scherrer lines into which they fuse (333).

A final decision in favour of one of these assumptions, or of a combination of them, cannot yet be made. Difficulties arise with the first two assumptions from the occasional absence of broadening [cf. also (339)]. Assumption 3, in so far as it admits of various types and distributors of the lattice disturbances, can give an account of this diversified behaviour of the metals.

On the basis of assumption 1 the magnitude of the elastic stress can be estimated from the broadening of the lines (change in the lattice constant), a procedure which would be inadmissible if assumption 3 applied. The values obtained in this way for the internal stress of copper after approximately 100 per cent. extension were about 6 kg./mm.^{2} for the single crystal, and about 13 kg./mm.^{2} for the polycrystal (334).

Since a displacement of a part of the lattice points from their normal position weakens the high-angle interferences more than the low-angle ones,[1] changes in the relative intensities of lines must also be expected as cold working increases. Actually it has been found that the intensity of a reflexion of higher order, compared with that of a lower order from the same plane, is smaller after cold working than in the unworked (annealed) state of the metal (Ta, Mo, W) (340). Systematic study of the changes in intensity which accompany deformation should afford a suitable method for a more detailed investigation of the accompanying disturbances.

60. *Cold Work and Physical and Chemical Properties*

Attention was drawn in Section 58 to the need for taking into account the changes in orientation when studying the physical and chemical properties of crystalline material after cold work. In this connection mention should be made of the internal cavities which occur in deformed metals, for instance in overdrawn wires, and which, of course, affect numerous properties (density, specific resistance, etc.). It has already been pointed out in Section 38 that purely crystallographic processes may be the cause of these internal cavities (Rose's channels, which accompany multiple twinning).

A summary of the changes produced by cold deformation in the physical and chemical properties of metals, omitting the obviously trivial effects, is contained in Table XXI. In conformity with the observed invariance of the lattice constants under cold working, which has already been described, *the changes in density* are only

[1] A previous deviation from the normal position involves a relatively greater disturbance for high-indexed planes (with small lattice spacings) than for low-indexed planes which succeed each other at wider intervals.

TABLE XXI

Change Produced by Cold Work in the Physical and Chemical Properties of Metals

Property.	Metal.	Deformation, %.	Change.	Literature.
Density	Al single crystal	alternate stressing	0	(341)
	,, ,,	27% stretched	0	(342)
	,, ,,	~40% ,,	within a margin of error of (±0·02%)	(343)
	Polycrystal	~40% ,,	−0·3%	(343)
	Fe ingot iron Carbon steels	>90%	−0·4%	(344)
	Armco-iron Carbon steels	compression	at rising pressure initially −0·1% followed by a further slight increase	(345)
	Armco-iron	77% rolled	−0·12%	(346)
	,,	4% stretched	−0·36%	(347)
	Steel	5% ,,	−0·51%	(347)
	Cu	60% hammered	−0·2%	(348)
		drawn	0	(349)
		60% drawn	−0·3%	(350)
		4% stretched	−0·13%	(347)
	W	substantially swaged and drawn	initially +0·5% then −2%	(351)
		,,	with a margin of error of (±0·3%)	(352)
	Bi	extruded wire	slight reduction	(353)
	α-Brass 91% Cu single crystal	70% compressed	+0·13%	(342)
	α-Brass 91% Cu polycrystal	70% compressed	no definite change	(342)
	85% and 72% Cu single crystals	simple glide	0(±0·002%)	(354)
	85% and 72% Cu single crystals	multiple glide	−0·03%	(354)
	63% Cu	4% deformed	−0·16%	(347)
Moduli of elasticity and rigidity	Fe single crystal	7·5% stretched	−3%	(355)
	Carbon steel	90% drawn	~0	(344)
	Substantial increases or decreases in several tests on polycrystalline material. Development of deformation textures disregarded.			(356) (357)

TABLE XXI (*continued*)

Property.	Metal.	Deformation, %.	Change.	Literature.
Thermal expansion	Fe ingot iron	50%	± 0·1%	(358)
	W	drawn	+11% (?)	(359)
	Bronze	50%	± 0·1%	(358)
Specific heat	Zn	?	± 0	(360)
	Fe ingot iron (up to 0·5% C)	up to 90%	~ 0	(361)
	Armco iron and steel (up to 0·6% C)	forged	+ 3%	(362)
	Ni	99·5% drawn	within the limits of experimental error of (±0·5%)	(363)
	W	94% drawn		
	Bronze (5–6% Sn)	up to 90%	~ 0	(361)
Internal energy	Al single crystal	~55% stretched	~0·11 cal./g.	(365)
	Polycrystal	~20% ,,	~0·10 ,,	
		~70% drawn	~0·11 cal./g.	(366)
	Cu polycrystal	~20% stretched	~0·07 cal./g.	(365)
		~70% drawn	~0·23 ,,	(366)
	Fe	stretched until necking occurred	0·02 up to 0·09 cal./g.	(364)
Heat of solution	W	substantial	within the limits of experimental error	(369)
Heat of combustion	W	99% swaged and drawn	within the limits of experimental error of (±1%)	(370)
Electrode potential	Cu	abraded sheets	16 (1) *	(371)
	Zn		2 (4)	
	Mo		1 (0)	
	Ag		20 (9)	
	Cd		9 (1)	
	Pb		2 (0)	

* The figures 16 (1) indicate that out of 17 tests the surface of the abraded sheet was less noble in 16 cases, and that of the untreated sheet less noble in only one case.

TABLE XXI (*continued*)

Property.	Metal.	Deformation, %.	Change.	Literature.
Rate of diffusion	Increases, sometimes considerable, have usually been obtained in numerous tests with polycrystalline materials; but decreases have also been observed. Effect of the solvent. Development of deformation textures hitherto disregarded. Cold working modifies considerably the capacity of crystals for etching.			(372) (344) (373) (374) (375)
Thermo-electric force (compared with annealed metal)	Al, Ni, Cu, Ag, Au	drawn and rolled	+20 to +60 . 10^{-8} V/° C.	(376); also for copper (377)
	Fe		$-35 . 10^{-8}$ V/° C.	
Specific electrical resistance	Fe	>90% drawn	+2%	
	Steels	—	has not been satisfactorily determined	(344)
	Armco	4% stretched	+0·96%	
	Smaller increase in resistance with increasing C content			(347)
	1·3% C	4·5% stretched	+ 0·29%	
	Ni	>99% drawn	+ 8%	(378)
	Cu	82% drawn	+ 2%	(379)
		40–80% drawn	+ 2%	(380)
		4% stretched	+ 1·5%	(347)
	Mo	99% drawn	+18%	(378)
	Ag	60% drawn	+ 3%	(380)
	W	99% drawn	+50%	(378)
	Pt	99% drawn	+ 6%	(378)
	α-Brass (63% Cu)	4·3% stretched	+ 1·6%	(347)
	(α + β)-Brass (57% Cu)	4·0% ,,	+ 1·0%	
Temperature coefficient of electrical resistance	Ni	>99% drawn	− 5%	(378)
	Mo		−16%	
	W		−35%	
	Pt		− 7%	
Thermal conductivity	Cu crystal	swaged	−73%	(381)

small. If the observed decrease of the density exceeds the extent of the change in the lattice constant, the explanation must be sought either in unobserved cavities, or in precipitations (from supersaturated solid solutions) initiated by cold working.

Owing to the generally substantial elastic anisotropy of the metal crystals (cf. Table XIX and Fig. 154) the observed changes caused by cold working in *Young's modulus* and the *shear modulus* can be evaluated only if the determinations are carried out on polycrystalline material. When performing these tests hitherto little account has been taken of the formation of deformation textures. In any case the available results show that the changes brought about in the elastic properties by cold deformation are only small.

A few important remarks have yet to be made regarding the change of the *energy content* of cold-worked metals. Sections 44 and 48 contain some figures for the mechanical energy of deformation taken up by various hexagonal crystals to the point of fracture. They were of the order of four to eighteen times the specific heat of the metal. Most of the energy of deformation is converted into heat; only a fraction (1–15 per cent.) remains as internal energy in the material [(364), (365), (366)]. Whether saturation with internal energy represents the physical condition of fracture for metallic materials, as has been surmised for steel on the basis of cyclic bending tests (367), and for copper and steel on the basis of static torsion and compression tests (368), is one of the basic problems of the theory of mechanical properties. In any case experiments show that the increase of internal energy diminishes as cold working progresses and a state of saturation is approached. The quantity of total energy of deformation, which leads to the saturation of copper with internal energy at 15° C. in the torsional test, amounts to slightly more than 14 cal./g. In the compression test, after approximately the same amount of *energy of deformation* has been taken up, no further increase of the compressive yield stress occurs in the course of further deformation. A first attempt to estimate what proportion of this internal energy is stored in the form of elastic stress energy appears to indicate that this is very small, being about 1 per cent. of the increase in the internal energy (382).

Exploratory experiments carried out on brass crystals give some idea of the connection between heat development and the mechanism of deformation (383). It was found that at each change in the mechanism of glide much more heat was liberated than during glide in one system (cf. the behaviour of density in Table XXI). The changes which occur in the specific resistance of the α-brass crystals

when worked in several stages are entirely analogous; they are closely related to the mechanism of deformation. In the region of simple undisturbed glide the changes in resistance are slight, despite appreciable hardening; the increase of the resistance becomes substantial (about 2 per cent.) as soon as disturbances of the glide process occur (384).

As will be seen from the changes given in the table for the *specific electrical resistance* (ρ) and its *temperature coefficient* (α), the product $\rho \cdot \alpha$ remains on the whole constant. The Matthiessen law, originally stated for the formation of solid solutions ($\rho \cdot \alpha$ const.), is thus confirmed for cold working also [(385), (378)]. This makes it possible to infer the change in the specific resistance from the temperature coefficient which can be reliably determined independently of the existence of internal cavities.

The *colour* and the *limits of resistance* of alloys to chemical attack can also be altered by cold working. For instance, Au–Ag–Cu alloys become distinctly yellower during cold working [(386), (371)]. The alloy-composition limits within which chemical attack becomes effective are modified by cold working, and their sharpness is reduced (387).

Changes in the *magnetic properties* have also been omitted from the table as they have not yet been investigated with sufficient care. The saturation of magnetization remains substantially unaltered by cold deformation, coercive force and hysteresis increase (3–4-fold), while the maximum permeability is greatly reduced (to approx. 1/3) [(344), (388)]. As regards magnetic susceptibility, metals and alloys can be divided into two groups; in the first group (Cu, Ag, Bi, Pb, the brasses) cold working increases the magnetic susceptibility of paramagnetic and decreases that of diamagnetic metals. Copper and the brasses even pass from the diamagnetic into the paramagnetic condition. With the metals of the second group (Al, Au, Zn, W, Mo, nickel-silver) there is practically no change in susceptibility [(389), (390) and especially (391)]. The most probable explanation of this behaviour, and one which is confirmed by ample experimental evidence, is that ferro-magnetic phases are precipitated by cold working—even in the case of the so-called pure metals—a phenomenon which is not observed in the unworked state at room temperature owing to the exceedingly small rate of nucleation. The metals of the first group possess low solubility of the ferro-magnetic phase at room temperature, the solubility increasing with temperature (391). Consequently the change in susceptibility is not a true change of a physical property explicable in terms of

electron theory, but a secondary effect of cold working which is mainly a consequence of atomic rearrangement processes.

Cold working is also very important for many other processes, the mechanism of which consists of atomic rearrangements in the crystal lattice. Among these are *phase transformations*, *diffusion* and *recrystallization*. Thus the transformation of β- into α-tin, and of β- into α-cobalt is greatly accelerated [(392), (393)]. The speed of self-diffusion in worked lead is greater by many orders of magnitude than in the undeformed single crystal (394). This accelerated diffusion is also confirmed by the numerous experiments on the ageing of metal alloys. The precipitations responsible for this very important technical process are greatly accelerated by cold working of the super-saturated solid solutions [cf. for example (395), (396)]. We might also include in this group of phenomena the change in the axial ratio of the tetragonal Au–Cu single crystals which occurs as a result of hammering (397), and the influence of pulverization on the atomic distribution and lattice constants of a Fe–Al alloy (398). The capacity for forming new grains (recrystallization), which increases with the degree of working, and which distinguishes the worked from unworked metal, will be dealt with separately in the next section.

In conclusion, attention is drawn to a classification, often attempted in recent years, of the properties according to how they are influenced by cold working (399). Properties which are substantially altered by cold deformation (and impurities) are termed *structurally sensitive* (represented mainly by the mechanical properties, specific resistance, atomic rearrangement properties), in contrast to the structurally insensitive properties (lattice dimensions, thermodynamic properties). Although this distinction is in many ways supported by the observed facts, the material in Table XXI shows the difficulty of establishing clear and unmistakable criteria.

G. RECRYSTALLIZATION

The changes brought about in the physical, chemical and technological properties of metal crystals and crystal aggregates by cold working are not usually permanent : *the strain-hardened condition of the crystal does not represent a state of equilibrium.* We have already considered recovery (Sections 49, 50, 54), a phenomenon as a result of which the altered mechanical properties gradually approach again their original values without the formation of new grains, and while still maintaining the orientation of the lattice. Indeed, in

certain cases the reversion is complete (100 per cent. recovery). Besides this gradual recovery, the hardened crystals can also return to the stable condition by a more radical method; as a result of the thermal agitation, new unhardened crystal nuclei develop individually, and, by absorbing the hardened crystal mass, produce an entirely new grain texture : *recrystallization*. This phenomenon is distinguished from crystal recovery by the discontinuity of the process in the individual crystal. The main physical principles underlying this " work recrystallization " will be discussed in the

FIG. 162.—Commencement of Recrystallization in the Glide Planes of Low-carbon Steel (402).

following section.[1] This will be followed by a brief reference to the " grain growth " referred to in Section 12, which also leads to a re-formation of the texture. The causes of this type of recrystallization differ fundamentally from those which govern work recrystallization. Grain growth occurs as a result of the surface energy striving towards a minimum.

61. *The Nature of the Recrystallization Nuclei*

In the same way as the cast texture which develops when the melt solidifies is determined by the number of the nuclei and the speed of their growth [according to Tammann (401)], so, too, the structure which results from work recrystallization depends upon the number of nuclei formed per second and the speed at which they continue

[1] See (400) for the historical development of research on recrystallization.

to develop. In the present section we will deal with the recrystallization nuclei.

Since the number of nuclei increases with the amount of cold work, other things being equal, it follows that they are points of very high energy content and not simply particles of crystals which have remained undeformed. This appears clearly from Figs. 162 and 163, which show the start of recrystallization along operative glide

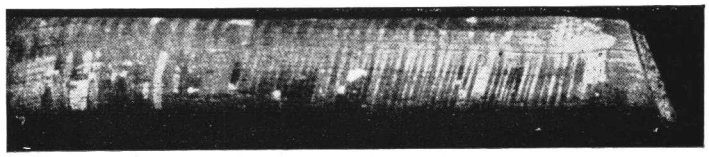

(*a*) Aluminium (cf. also 403).

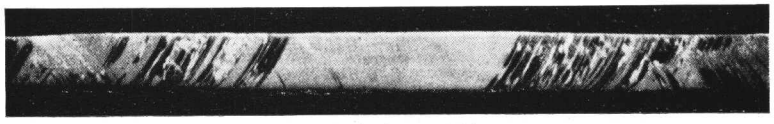

(*b*) Cadmium (417).

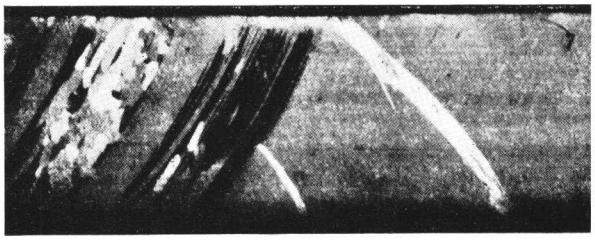

(*c*) Cadmium : section from (*b*).

FIG. 163 (*a*)–(*c*).—Recrystallization in the Twin Lamellæ.

planes and in deformation twins. The tendency for recrystallization nuclei to occur in deformation twins is very noticeable. For instance, recrystallization always occurred in the twin lamellæ of extended cadmium crystals after annealing for 1 minute at temperatures of 145° C. and upwards; on the other hand, in the area free from twins new grain was observed to form only at temperatures above 240° C.

The magnitude of deformation is of secondary importance only; thus with tin crystals a compression by a few per cent. produces recrystallization more readily than an extension by many hundreds

per cent. (404). It is plausible to connect the capacity for recrystallization with the hardening resulting from deformation. Hardening, too, is much more pronounced in a compressed crystal interspersed with numerous twin lamellæ, than in a crystal in which stretching has allowed the mechanism of glide to operate freely.

An exact investigation of the connection between hardening and the recrystallization texture was carried out on polycrystalline aluminium (405) and tin (406). The simple fact was established that, after stretching and recrystallization, the same grain size in the various samples always accompanied the same hardening. Fig. 164 shows this for aluminium; samples of strips having a substantially different initial grain size were subjected to the same operative stress before annealing. The number of nuclei increases with the degree of hardening. It is true that for single crystalline material the effective stress attained cannot be adduced as a measure of hardening, owing to the marked dependence of the yield point and the stress–strain curve on orientation. In this case it would have been necessary to deform until the operative glide elements had attained an equal degree of shear hardening, *i.e.*, up to the same point on the yield–stress curve. Experiments of this nature with the aluminium crystals have revealed the interesting fact that it is not unimportant whether the same hardening results from glide on only one or on two equivalent systems. In the second case the capacity for recrystallization is greatly reduced (see Fig. 165). With the single crystal, therefore, it is possible in the normal tensile test for more pronounced hardening to be accompanied by a reduced capacity for recrystallization. Consequently in this case hardening is not a valid measure for the capacity for recrystallization. The same result emerged from tests carried out on tin crystals. If

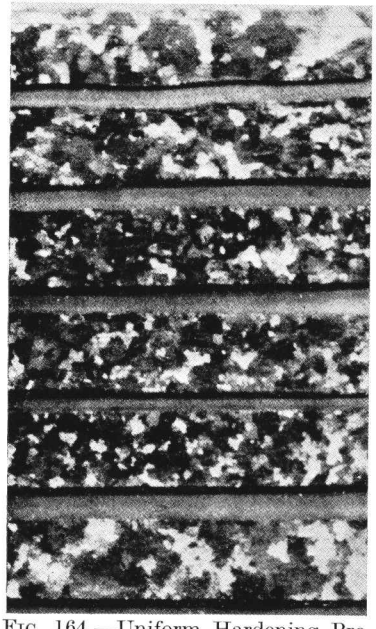

FIG. 164.—Uniform Hardening Produces Uniform Grain Size of the Recrystallized Texture. Al Polycrystal (407).

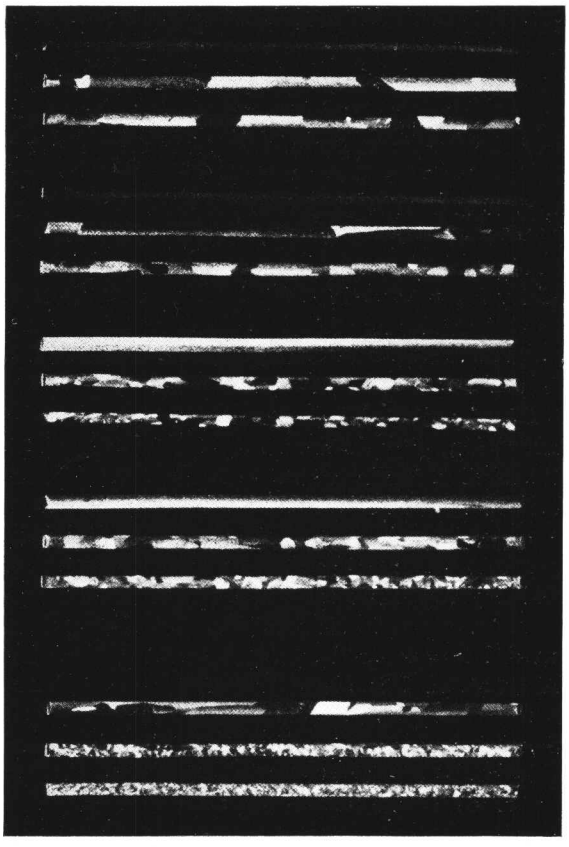

FIG. 165.—Recrystallized Al Crystals. Diverse Grain Size after Identical Hardening (408).

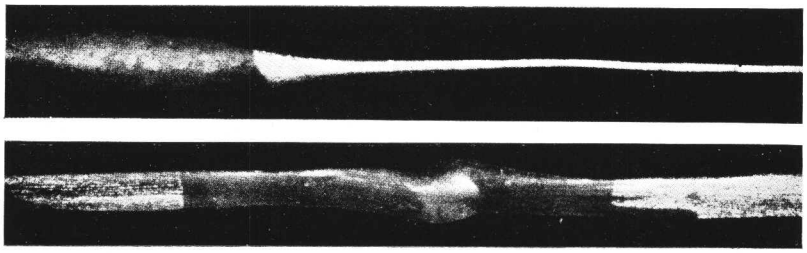

FIG. 166.—Recrystallized Sn Crystals. Formation of Nuclei in the Transition Zones between Stretched and Unstretched Parts (404).

crystals taken from substantially stretched and from unstretched parts are annealed at low tempreature (150° C.), it is observed that nuclei always form in the transition zones (Fig. 166), while maximum hardening is certainly exhibited by those parts which have been substantially stretched.[1] Aluminium crystals subjected to plastic torsion followed by reverse torsion revealed that the capacity for recrystallization, like the X-ray asterism, was greatly reduced after the deformation had been reversed, although hardening remained unaffected (403; cf. also 410). Special attention was given to the case of bending and back-bending. Here, too, a marked reduction in the capacity for recrystallization after reverse deformation was observed, notwithstanding this had further increased hardening (measured by the hardness of the aluminium crystals) (411).

Although the results obtained with single crystals show that there is no direct connection between hardening and the capacity for recrystallization, they do not weaken the assumption of a more fundamental relationship between the tendency towards recrystallization and the increased internal energy which results from deformation. One may, indeed, conjecture that this internal energy is reduced by reverse deformation, since by this operation the elastically distorted glide layers are substantially re-straightened, and so regain their elastic stress-energy. Since it was also observed that reverse deformation did not proceed along the same glide planes as the original deformation, but along planes which lie between them (412), it is not necessary to assume the presence of strong local accumulations of energy on those glide planes which were originally operative. Moreover, after reverse deformation, the crystal may revert to a more stable condition by recovery. But previous recovery reduces the capacity for recrystallization, and may even eliminate it. In transition zones and at the junctions of irregularly extended crystals where macroscopically different lattice positions adjoin each other, such complete recovery can never occur. The reduced capacity for recrystallization after several glide systems have become operative is also understandable in the light of the above; an increase in the number of disturbed areas in the lattice,

[1] Recrystallization is much more difficult to produce in extended tin crystals without visible glide bands than in those with glide bands. They recrystallize only just below melting point, small irregularities in the crystal serving as nuclei (404). The experiments which failed to confirm the formation of nuclei in the transition zone described above were obviously carried out on such crystals without glide bands (409). The causes of this different behaviour of the two types of tin crystals, a difference which is also reflected in the magnitude of the extension which can be achieved, have not yet been elucidated (it is possibly due to small variations in the degree of purity).

but a decrease in the extent of the disturbance after double glide, leads to the same hardening as simple glide, but it reduces the number of nuclei (408).

The fact that in many cases the hardening which occurs in the polycrystal can serve as a quantitative measure of the capacity for recrystallization,[1] does not conflict with the results obtained with single crystals. Annealing of the deformed polycrystal reveals merely an average capacity for recrystallization, from which the differences between the variously oriented grains cannot be recognized—all the more so since the effect of the grain boundaries tends to eliminate the individual differences. As a result of the differing orientations of adjacent grains very strong distortions (hardening) occur in the neighbourhood of the grain boundaries, leading in this case to a marked increase in the number of nuclei (Fig. 167). Consequently the smaller the initial grain size, the

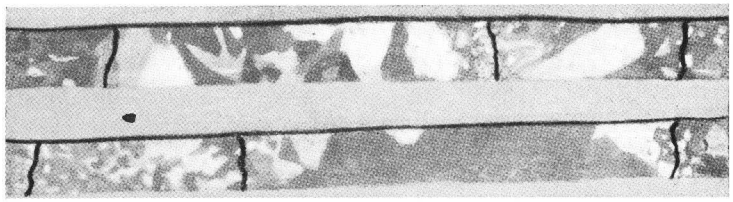

FIG. 167.—Increase of Nuclei in the Vicinity of the Grain Boundaries. Al (405).

smaller are the grains after recrystallization for the same degree of deformation [(405), (414)].[2] With decreasing temperature of working and constant degree of working (increased hardening), the recrystallized grain size becomes finer; the number of nuclei increases as the annealing temperature is raised (415). This behaviour is disturbed if a subsequent grain growth cannot be separated from the work recrystallization [example, aluminium of high purity (416)].

All the experiments, therefore, point to the recrystallization nuclei as being regions of maximum energy accumulation. In many cases where deformation is uniform there will be a parallel increase of internal energy and hardening. In that case the resultant hardening is a measure of the capacity for recrystallization.

[1] Nevertheless, even with extended polycrystalline aluminium specimens a reduction of the capacity for recrystallization was observed after reverse straining (compression) (increase in the temperature of recrystallization) (413).

[2] This is paralleled by the fact that the extension of single crystals occurs as undisturbed glide even at temperatures at which the extension of the polycrystal is attended by constant recrystallization (see Section 48).

62. *Velocity of Growth of the Newly Formed Grains*

We have stated the grounds for supposing that the nuclei for the formation of new grain in work recrystallization coincide with the areas of maximum energy accumulation. In this section we will

TABLE XXII

Recrystallization of Extended Metal Crystals. Speed of Growth of Newly Formed Grains

Metal	Annealing temperature, ° C.	Mean speed of growth (mm./sec.) in successive intervals of				
		5–10.	5–10.	5–20.	5–30.	60.
		Seconds.				
Tin, extended by about 400% (404)	160	0·46	0·32	0·15	0·1	0·1 *
		2·7	1·7	1·1	0·13	—
	220	3·2	—	—	—	—
		2·1	—	—	—	—
		1·7	0·76	0·71	—	—
		Intervals of				
		30.	120.	300.	600.	4800.
		Seconds.				
Aluminium extended under a stress of up to 4 times that of the yield point (0·2% permanent set) (417)	520	0·022	0·028	—	—	—
		0·045	0·028	—	—	—
		No visible grains	>0·028	0·017	0·0007	—
			>0·031	0·019	—	—
			>0·022	0·009	—	—
			>0·022	0·002	—	—
			>0·019	0·009	—	—
			>0·011	0·012	0·006	—
			>0·014	0·011	—	—
			>0·011	0·007	—	—
		0·078 †	0·039	0·018	0·0006	—

* A dash indicates that no further growth of the crystal was observed during the particular interval.

† This crystal was stretched at a stress corresponding to only 3 times that of the yield point.

discuss the *speed of the growth* of the recrystallization grains which have developed from the recrystallization nuclei. That the newly formed crystals are mainly in the unhardened, stable condition is apparent from an investigation of their plastic properties, which

correspond to those of undeformed crystals, and from the X-ray diagrams which show no signs of lattice disturbance.

It is often possible (if the formation of the nucleus is localized) to recrystallize a deformed crystal very largely as a single crystal. In the process the lattice of the newly formed crystal, regardless of the lattice orientations in the deformed crystal, grows parallel to itself, as has been found in tests carried out on extended and subsequently twisted tin crystals (404). The figures contained in Table XXII convey some idea of the magnitude of the speed of growth in the recrystallization of single crystals; they relate to tin crystals which had been stretched to flat ribbons, and to sheet-

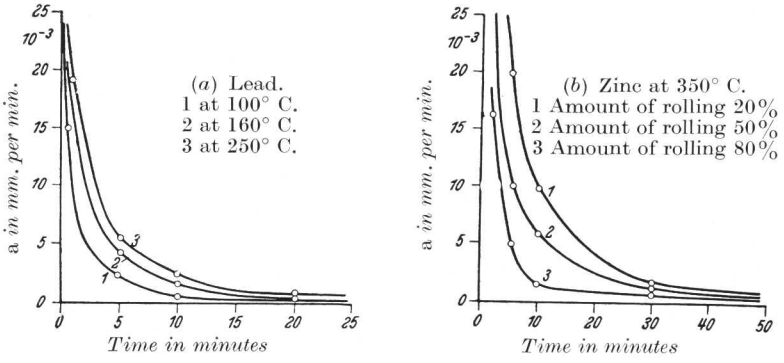

FIG. 168 (*a*) and (*b*).—(*a*) Speed of Recrystallization (*a* in mm./min.) as a Function of Temperature, and (*b*) Degree of Deformation (418).

shaped aluminium crystals, each of which had been deformed up to definite stresses. As will be seen from the figures in the table, the velocity of growth falls away in each case with increasing duration of the annealing period; often the growth of the new crystal comes to a complete standstill after a short time.

Similar results were obtained also with polycrystalline specimens of lead, silver and zinc. The speed of grain-boundary displacement as a function of the annealing period is given for various annealing temperatures and degrees of deformation in Fig. 168. The decrease in rate of grain growth was thought to be caused by the precipitation of impurities at the grain boundaries.[1]

We think that attention should also be directed to the recovery which precedes recrystallization and which leads, without the

[1] When an unstable phase type is transformed into a stable one the velocity of the grain-boundary displacement is independent of the time.

formation of new grain, to a smoothing of the lattice disturbances (a very substantial effect in the case of a uniformly oriented deformed single crystal), and so to a reduction of the capacity for recrystallization.

In contrast to the above cases, measurements on polycrystalline aluminium revealed that the newly formed grains grew at a uniform speed (420).

The maximum velocities of growth at the start of the annealing of a deformed single crystal (see Table XXII) exceed many times

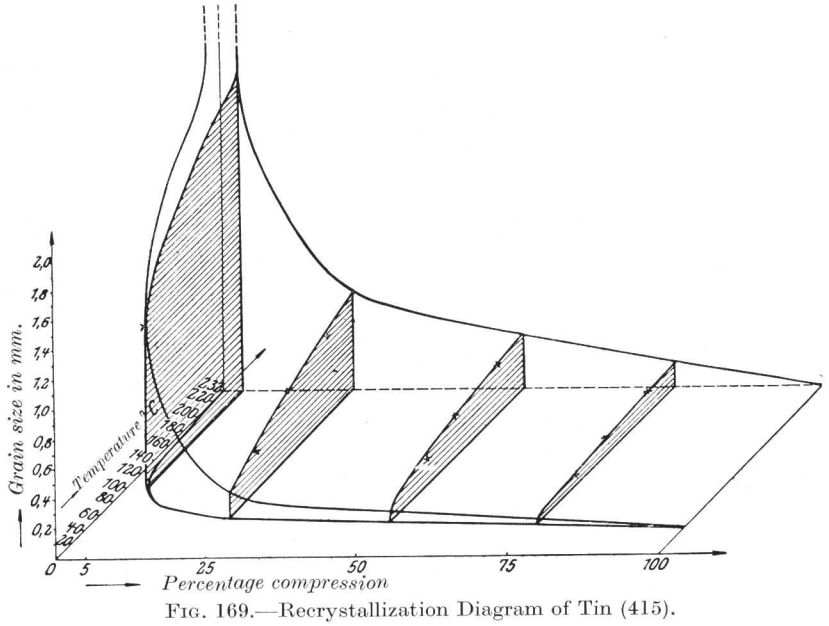

FIG. 169.—Recrystallization Diagram of Tin (415).

the speeds observed for the recrystallization of polycrystals. Thus for polycrystalline tin (annealing temperature 100° C.) a linear speed of growth of about 0·17 mm./sec. is obtained (419), while for aluminium (deformation 10 per cent., annealing temperature 370° C.) it is about 0·0007 mm./sec. (420). An explanation of all these very striking discrepancies between the behaviour of single crystal and polycrystal cannot be given at present; all the more so as the test conditions (degree of purity of the metal, plastic strain, annealing temperature) were by no means identical in the various tests. Nor can an answer yet be given to the question whether the great speeds observed in the single crystal are in any way connected with the

relations between the orientations of the consuming and the consumed crystal (cf. also Section 63).

The results of comprehensive research into the dependence of the velocity of growth on the plastic strain and the temperature of annealing are available for polycrystals only. They show that the velocity decreases with both decreasing strain and annealing temperature. This decrease leads even at finite deformations to a zero value, which means that there is a limit of deformation below

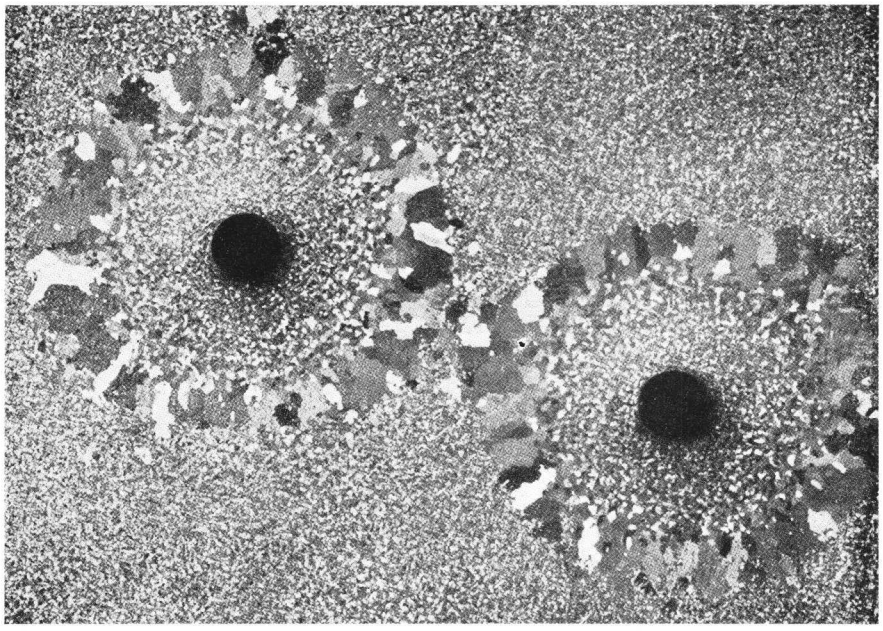

FIG. 170.—Bullet-holes in an Annealed Sn Sheet (415).

which no appreciable work recrystallization occurs even at the maximum temperature attainable [(415), (405), (406)].

As a result of the dependence of the number of nuclei and the velocity of growth on the plastic strain and annealing temperature there is naturally also a connection between these two variables and the grain size of the texture which arises after recrystallization. This relationship, which can be determined empirically, is represented by the *Recrystallization diagram* [Czochralski (419)]. As an example, the recrystallization diagram of tin is shown in Fig. 169. The general principles underlying such diagrams are, that at a given

annealing temperature the grain size diminishes with increasing plastic strain, and increases for a given plastic strain with increasing temperature of annealing. Fig. 170 illustrates the first principle very clearly by a tin sheet which had been shot through and subsequently recrystallized (fine grain in the immediate vicinity of the holes, increase in grain size with distance from the holes, no recrystallization beyond the zone of coarse grains).

In this context it is important to observe that the new grains formed by recrystallization lose their capacity for further growth into the deformed material immediately they experience the slightest permanent deformation [(406), (405)]. Fig. 171 demonstrates this statement very clearly. The initial aluminium sheet had two lateral incisions in order to localize the recrystallization produced by slight stretching. After several large crystals had formed round the base of the notches, four more incisions were made (electrolytically, in order to avoid deformation), as is seen in Fig. 171*a*). These enabled a part of the sheet to be stretched while other parts remained undeformed. After annealing it was found (Fig. 171*b*) that those parts of the crystals which had remained undeformed continued to grow, while the recrystallization in the deformed parts had stopped. Slight deformation, even if it remains below the limiting value for recrystallization, deprives the newly formed crystal of the capacity to grow at the expense of the deformed environment.

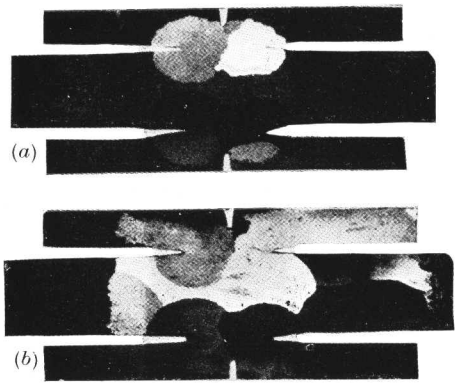

FIG. 171 (*a*) and (*b*).—Loss of Capacity for Growth of a Newly Formed Grain as a Result of Slight Deformation. Al (421).

(*a*) At this stage the centre portion is slightly stretched; (*b*) After heating the large grains grow only in the undeformed lateral strips.

63. *Orientation of the Newly Formed Grains*

The orientation of the newly formed grains, as well as the number of nuclei and the velocity of growth, are significant in the study of work recrystallization. It has already been remarked in the case of extended *tin* crystals which, through recrystallization, had again

become single crystals, that certain relationships existed between the orientations before and after annealing [(422), (404)]. This was shown by the fact that, if the crystal was extended afresh, the original plane of the ribbon was usually retained, and the new glide striations adopted a position related to that resulting from the first extension. In nineteen out of thirty-five cases investigated the subsequent extension of the crystal was found to retain the initial ribbon plane.

The orientation relationships have been very thoroughly investigated for *aluminium*. If the plastic strain of the crystals was so small that only one or very few new crystals could form in the course of recrystallization, no relationship could be found between the initial orientation and the orientation of the recrystallized grains [(423), (424)]. Where the number of grains produced from the stretched single crystals is somewhat greater (10–30), a preference, though only a slight one, for the orientation of the mother crystal was found. There were also indications of an influence of the direction of deformation, despite the very considerable scatter of the positions of the crystallites (425). Heavy deformation of the crystals (rolling down to one-quarter of the thickness) followed by annealing at 600° C. (for a few seconds only, in order to avoid grain growth) leads to a recrystallization texture that is related to the deformation texture (after rolling) in an entirely reproducible manner. In some cases there is only a slight scatter between recrystallization texture and rolling texture, while in others the two textures diverge appreciably. By altering the direction of rolling in the original crystal, not only the rolling texture but also the arrangement of the new crystals after work recrystallization is changed (426). As in the rolling of aluminium crystals, so in their plastic compression down to approximately one-third of their thickness, regular relationship is observed between the compression texture and the recrystallization texture arising after short annealing at 600° C. [(427), (428)]. The newly formed crystals show preferred orientation which arises from the principal orientation of the deformation texture through the rotations (20–60°) connected with the process of glide, and described in Section 59. Where double octahedral glide becomes operative the orientations of the recrystallization texture are doubled compared with the deformation texture after compression and rolling. It would therefore appear as though those parts of the lattice which had rotated out of the main position, and so become especially distorted, represented favourable nuclei for recrystallization.

Investigations into the recrystallization of other metal crystals are hardly available. Yet it is precisely such research which would be of the greatest importance for our knowledge of the recrystallization textures of deformed technical components after annealing (see Section 80).

64. *Grain Growth*

The three preceding sections contain the limited information available to-day about the recrystallization of single crystals after cold deformation. Although it has been possible to establish certain fundamental laws of work recrystallization, numerous questions have still to be answered, in particular those connected with orientation relationships. No less obscure are the phenomena connected with grain growth (secondary recrystallization, boundary migration). This consists in a subsequent, irregular and very much slower process which, after appreciable cold deformation, and if heat treatment is continued, follows the work recrystallization and may result in extremely different grain sizes and shapes.

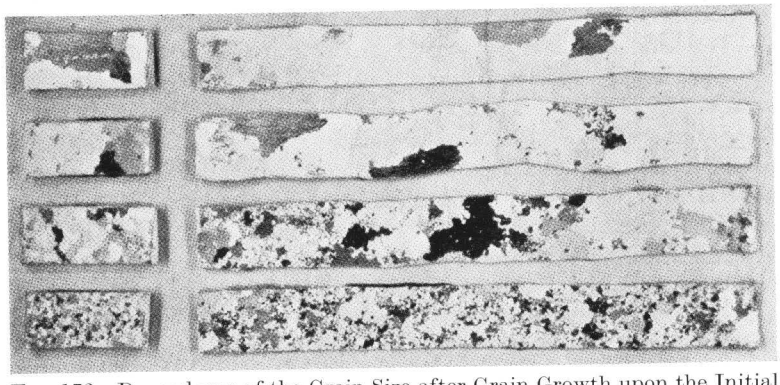

FIG. 172—Dependence of the Grain Size after Grain Growth upon the Initial Grain Size. Al (416).

Aluminium, which was used in the investigation of work recrystallization, was also mainly employed for the study of grain growth. In the first place it was discovered that, provided cold deformation is not carried too far, a clear connection exists between initial grain size and the grain size after completed grain growth. This will be seen from Fig. 172, which shows strip specimens of varying initial grain size which were subjected to prolonged heat-treatment at 600° C. after rolling down to about one-quarter of the original